Environ. Sci. Technol. **2004**, *38,* 5505−5513

Atmospheric Dry Deposition of Persistent Organic Pollutants to the Atlantic and Inferences for the Global Oceans

ELENA JURADO,[†] FODAY M. JAWARD,[‡] RAINER LOHMANN,[‡,||] KEVIN C. JONES,[‡] RAFEL SIMÓ,[§] AND JORDI DACHS*[,†]

Department of Environmental Chemistry, IIQAB-CSIC, Jordi Girona 18-26, Barcelona 08034, Catalunya, Spain, Environmental Science Department, Lancaster University, Lancaster LA1 4YQ, U.K., and Marine Sciences Institute, CMIMA-CSIC, Passeig Marítim de la Barceloneta 37-49, Barcelona 08003, Catalunya, Spain

Atmospheric deposition to the oceans is a key process affecting the global dynamics and sinks of persistent organic pollutants (POPs). A new methodology that combines aerosol remote sensing measurements with measured POP aerosol-phase concentrations is presented to derive dry particulate depositional fluxes of POPs to the oceans. These fluxes are compared with those due to diffusive air−water exchange. For all polychlorinated biphenyl (PCB) congeners and lower chlorinated dibenzo-*p*-dioxins and furans (PCDD/Fs), air−water exchange dominates the dry deposition mechanism. However, this tendency reverses in some areas, such as in marine aerosol influenced areas and dust outflow regions, consistent with the important variability encountered for the depositional fluxes. Seasonal variability is mainly found in mid-high latitudes, due to the important influence of wind speed enhancing dry deposition fluxes and temperature as a driver of the gas-particle partitioning of POPs. The average dry aerosol deposition flux of ΣPCBs and ΣPCDD/Fs to the Atlantic Ocean is calculated to be in the order of 66 ng m^{-2} yr^{-1} and 9 ng m^{-2} yr^{-1} respectively. The total dry aerosol deposition of ∑PCBs and ∑PCDD/Fs to the Atlantic Ocean is estimated to be 2200 kg yr^{-1} and 500 kg yr^{-1}, respectively, while the net air−water exchange is higher, 22000 kg ∑PCBs yr^{-1} for PCBs and 1300 kg ∑PCDD/Fs yr^{-1}. Furthermore, it is suggested that marine aerosol plays an important role in scavenging atmospheric contaminants.

Introduction

After being emitted or revolatilized, persistent organic pollutants (POPs) partition between the gas and aerosol phases and are subject to long-range atmospheric transport (LRAT). Semivolatile organic compounds may then be removed from the atmosphere to the ocean by three main processes: dry deposition of particulate-bound pollutants, diffusive gas exchange between the atmospheric boundary layer (ABL) and the surface ocean, and scavenging by rain (either from gas or particulate phases). Atmospheric depositional processes play a key role in the transport and fate of POPs at the regional and global scale (*1*−*8*). Furthermore, dry aerosol and gaseous deposition contribute to aquatic ecosystems pollutant burden and support POP accumulation in aquatic food webs (*9*, *10*). Previous reports comparing the different removal mechanisms show that diffusive air−water exchange dominates over wet and dry particle deposition for POPs predominantly found in the gas phase, except in rainy regions and close to urban areas with high concentration of atmospheric particulate matter. Conversely, dry particle deposition is important for chemicals that have a strong affinity to aerosols such as polycyclic aromatic hydrocarbons (PAHs) (*11*).

Generally, reported measurements of POP atmospheric deposition refer to local ground-based measurements. There are very few studies dealing with remote and pristine oceanic regions (*12*), even in the remote areas characterized by elevated concentrations of aerosol, such as the Saharan dust outflow over the eastern Atlantic Ocean. Considering the lifetime of aerosol distributions and the important temporal and spatial variability associated to deposition and air−water exchange, it is clear that simple extrapolations to derive large scale estimations of both fluxes from these local measurements could introduce an important bias in the estimation. In this context, satellite retrieval data of aerosol characteristics provides valuable information that allows a synoptical view of biogeophysical variables and can be used to estimate deposition at the regional and global scale. The first aerosol data from remote sensing were obtained in the mid-1970s. Important technical improvements have been made since then, triggered by studies of the influence of aerosols on climate change. Recent advances in space-borne instruments allow derivation of not only the aerosol concentrations but also parameters characterizing their size distributions (*13*). It is therefore now possible to assess the spatial and temporal variability and significance of dry aerosol deposition and air−water exchange of POPs at the global scale.

In short, the goals of this study are to (i) use remote sensing data from sensors designed to monitor aerosol distributions to predict dry deposition velocities of aerosols and aerosol-bound POPs at the global scale; (ii) develop a methodology to estimate the spatial and temporal variability of dry deposition of POPs for the Atlantic Ocean, derived from atmospheric measurements of gas- and aerosol-phase POP and from satellite data; and (iii) assess the relative importance of dry particle deposition and air−water exchange for the Atlantic Ocean and at the global scale. It is believed that the techniques developed here and their applications can contribute to an improved understanding of atmospheric depositional processes at the regional and global scale, an issue of increasing concern (*14*, *15*), and to help predict future trends of global POP fate under different climatic scenarios.

Field Measurements and Data Sources

Cruise Data. This work is based on atmospheric ship-board air concentrations of two representative families of POPs; polychlorinated dibenzo-*p*-dioxins and furans (PCDD/Fs) and polychlorinated biphenyls (PCBs). Data were obtained during two north−south Atlantic Ocean transects. PCDD/Fs were measured in air sampled on board the *RRS Bransfield* during an Atlantic cruise from the U.K. to Antarctica in October−December 1998 (52° N, 1° E−75° S, 20° W) (*16*). The PCB data were collected between The Netherlands and South Africa in January−February 2001 on board the *RV*

* Corresponding author e-mail: jdmqam@cid.csic.es.
[†] IIQAB-CSIC.
[‡] Lancaster University.
[§] CMIMA-CSIC.
[||] Current address: Research Center for Ocean Margins, Universität Bremen, D-28334 Bremen, Germany.

10.1021/es049240v CCC: $27.50
Published on Web 09/29/2004

Pelagia (52° N, 1° E − 34° S, 20° E) (*17*). Gas- and aerosol-phase POP concentrations were obtained from high volume samplers. In the case of PCBs, only gas-phase concentrations were determined, since PCB concentrations in the aerosol phase were below the detection limit. Latitudinal profiles of PCDD/Fs showed variability, with higher gas-phase values at low latitudes than at mid-high latitudes. PCBs present were detected throughout the cruise; the highest gas-phase detected values were found around 10° N and for samples where the air mass came from land. Both compounds displayed a gradient with concentrations decreasing from the northern hemisphere (NH) to the southern hemisphere (SH). Details of the methods, data variability, and trends are given elsewhere (*16*, *17*) and in the Supporting Information (Annex I).

Satellite Data. Meteorological Variables: Sea Surface Temperature and Wind Speed. Sea surface temperatures (SST) were obtained from the Along Track Scanning Radiometer (ATSR) on the European Space Agency ERS-2 satellite (ATSR project Web page http://www.atsr.rl.ac.uk). SST images consist of monthly averaged skin layer temperatures with a resolution of a half degree and an accuracy of ±0.3 K. Temperatures in the air film layer adjacent to the sea surface have been assumed the same as SST. Monthly global wind speed distributions were obtained from the NOAA special sensor microwave/imager (SSM/I) at a resolution of 1° × 1° and an accuracy ±2 m s^{-1} (http://lwf.ncdc.noaa.gov/oa/satellite/ssmi). There is a lack of these estimations in latitudes close to the poles, depending on the ice coverage. The data used correspond to monthly mean values for the period of field sampling—November 1998 or January 2001.

Aerosol Data. Aerosol parameters were obtained from the Moderate-Resolution Imaging Spectrometer Instrument (MODIS, http://modis.gsfc.nasa.gov/) on board the Terra satellite, part of NASAs Earth Observing System (EOS). Since MODIS remote sensing parameters for aerosol data were not available before mid 2001, climatological means for November and January of two consecutive years (2002, 2003) were used. Monthly climatological means of level 3 aerosol products such as the effective radius (r_{eff}, μm), its standard deviation (log(σ_{eff}), logμm), the aerosol optical depth (AOD), and the fine (submicron size) mode fraction (η) have been used (http://daac.gsfc.nasa.gov/data/dataset/MODIS/ 02_Atmosphere/02_Level_3). The advantage of MODIS retrieved data over other sensors is the information on aerosol size parameters. MODIS measurements of r_{eff}, log(σ_{eff}), η, and AOD are integrated over the air column, for the aerosol size range detected by the instrument (aerosol diameters from 0.1 to 20 μm) and with a resolution of 1° × 1°. They have an approximate accuracy of ±0.1 μm for r_{eff}, 25% for η, and ±0.03 ± 0.05*AOD for the AOD (*18*). Uncertainty is higher in regions with possible cloud contamination, over ice cover and over coastal areas and marshes. In dust regimes retrieved size parameters (r_{eff}, log(σ_{eff})) can underestimate up to about 40% (*19*, *20*) of the actual aerosol size.

Model Development

Dry Aerosol Deposition Flux. Experimental measures of dry aerosol deposition fluxes (F_{DD}, pg m^{-2} d^{-1}) are scarce and fluxes are often estimated by

$$F_{DD} = v_D \times C_p \quad (1)$$

where v_D is the overall aerosol dry deposition velocity (m d^{-1}) and C_P is the POP aerosol-phase concentration (pg m^{-3}) (*4*, *21*). v_D values are strongly dependent on aerosol size distribution, atmospheric turbulence (as influenced by wind speed), and at low wind speed by atmospheric stability. Pioneering studies that parametrized dry deposition velocities over natural surface waters, such as the models of Williams (*22*) and Slinn and Slinn (*23*), still provide useful and widely used synopses for estimating v_D values (*24*−*28*). This study has been based on the widely used Williams parametrization (*22*), which determines v_D values as a function of aerosol diameter, wind speed, and atmospheric stability. Additionally, it includes effects of spray formation under high wind speed conditions and particle growth due to high relative humidities. Previous studies have shown that dry deposition flux estimations from a distribution of aerosol size derived v_D values are more accurate than using a single overall v_D value (*29*, *30*). Therefore, assuming the aerosol size distribution is known, the aerosol diameter range is divided into a number of intervals (i), so that the total flux is given by

$$F_{DD} = \sum_i (v_{D,i} \times C_{p,i}) \quad (2)$$

where $v_{D,i}$ (m d^{-1}) is the deposition velocity for an atmospheric particle with a diameter in the midpoint of the interval i and $C_{p,i}$ (pg m^{-3}) is the corresponding POP concentration in the particle phase.

Aerosol size distribution over the oceans can be determined from the remote sensing measurements of aerosol r_{eff}, which is defined as the weighted integral of the volume-to-surface ratio, and log(σ_{eff}) mentioned above. Assuming the size distribution is log-normally distributed, which is a common assumption for remote homogeneous aerosols (*18*, *31*, *32*), r_{eff} and log(σ_{eff}) can be related to the median radius (r_g, μm) and the geometric standard deviation (log($\sigma_{r,g}$) logμm) (*33*) by

$$r_{eff} = r_g \exp\left(\frac{5 \log^2(\sigma_{r,g})}{2}\right) \quad (3)$$

$$\log^2(\sigma_{eff}) = \exp(\log^2(\sigma_{r,g})) - 1 \quad (4)$$

Once the parameters rg and log($\sigma_{r,g}$) are determined, the mass fraction of aerosols of size midpoint i (w_i, dimensionless) to total suspended particulate matter values (TSP, kg m^{-3}) can be derived as described in Annex II (Supporting Information). In this study, 6 intervals of aerosol diameters have been considered among the range available from MODIS on the Terra satellite (D_{min}-D_{max} (μm): 0.1−0.6, 0.6−1, 1−2, 2−3, 3−5, 5−20). Figure 1 shows TSP and two characteristic distributions of w_i for the Atlantic Ocean. The distribution of size fractions suggests that most of the aerosol mass is predominantly accounted for aerosols with diameters between 1 and 2 μm, even though the highest number of concentrations occur in the range 0.1−1 μm. The former range of sizes accounts for an important part of the plume resulting from dust in the Saharan desert (20−25° N) and from the Sahel region (10−15° N) of northern Africa, flowing across the Atlantic toward the Sargasso and the Caribbean Seas. Increased loadings of submicron aerosols are found during some months, close to industrialized countries in the northern Atlantic and in smoke biomass burning areas such as west-central Africa. Interestingly, submicron particles and aerosols in the range 1−3 μm are found over the southern mid-latitudes, which can be attributed to marine aerosol, i.e., salt particles emitted from bursting sea foam during windy conditions.

POP distribution to aerosols of different sizes needs to be accounted, but different studies give different size distribution information, and no assessment exists for the oceanic atmosphere (*34*). For example, some authors suggest higher POP concentrations in submicron aerosols (*35*, *36*), while other find different aerosol size distributions of POPs (*37*−*40*). Therefore, POP concentration has been assumed to be uniform over the size spectrum of aerosols. The influence of this assumption is discussed below.

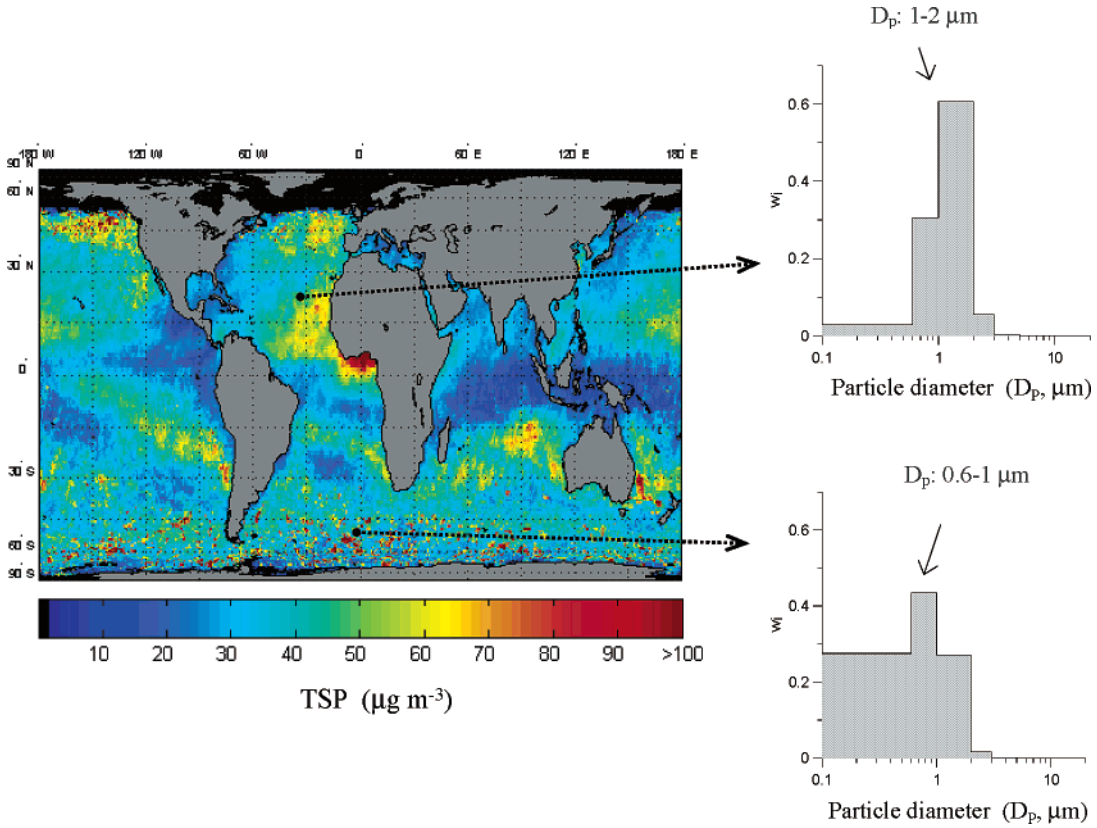

FIGURE 1. Aerosol concentrations over the surface ocean (TSP, μg m^{-3}) derived from the aerosol optical depth given by MODIS. Values from climatological January 2002−2003. Aerosol size distribution (w_i) are shown for characteristic oceanic regions (in Peters Projection of the world: equal area presentation).

Therefore, the POP concentration in aerosol size i ($C_{p,i}$) is proportional to the mass fraction of particles in the interval (wi, see Annex II) and F_{DD} is given by

$$F_{DD} = \sum_{i=1}^{6}(v_{D,i} \times w_i \times C_p) = C_p \times \sum_{i=1}^{6}(v_{D,i} \times w_i) \quad (5)$$

and the overall mass averaged dry deposition velocity (v_D) is given by

$$v_D = \sum_{i=1}^{6}(v_{D,i} \times w_i) \quad (6)$$

Estimates of v_D are parametrized as described by Williams (*22*), and therefore $v_{D,i}$ values for the different aerosol sizes i can be determined. These $v_{D,i}$ values show a strong dependence on wind speed, especially for small aerosols (<1 μm) where turbulent diffusion becomes a dominant mechanism. Wind speed has a nonlinear influence on dry deposition. Monthly averaged wind speeds have therefore been corrected by taking into account the Weibull distribution of wind speeds over oceanic regions (*41*). The resulting dry deposition velocities ($v_{D,i}$) are increased 20%, on average, due to nonlinear influence of wind speed, but this effect is very sensitive to aerosol size. Methodological details of the derivation of $v_{D,i}$ are given in Annex III (see Supporting Information).

Figure 2 presents a global map of the overall dry deposition velocity over the oceans, in January 2002−2003. It shows significant spatial variability, where raised values are related to either high wind speeds (such as in mid-high latitudes of the northern and southern hemispheres) or larger fractions of mass concentration of coarse aerosols (>1 μm). v_D values range from 0.01 cm s^{-1} to 0.8 cm s^{-1}. These values are comparable to those reported in previous studies of particle deposition velocities in coastal or lake environments (*21*, *42*), or modeling studies (*26*), which usually range from 0.1 to 0.8 cm s^{-1}. However, a notorious spatial variability of v_D values occurs. As noted earlier, MODIS characterization of aerosols fails to fully account for the importance of dust aerosols in desert outflow regions, and therefore it is possible that v_D values are underestimated in some regions such as the Sahel-Saharan outflow over the Atlantic Ocean.

Predicted Gas-Particle Partitioning of PCBs. For PCDD/Fs, both gas- and aerosol-phase concentrations for the Atlantic Ocean transect were measured (*16*). However, in the case of PCBs, it was necessary to infer the particle-phase concentration from the measured gas-phase concentration, since it was not measured during the 2001 sampling campaign as described above. This can be done by (*43*)

$$C_P = C_G \times TSP \times K_P \quad (7)$$

where C_G is the gas-phase concentration (pg m^{-3}), and K_P (m^3 kg^{-1}) is the particle-gas partition coefficient. The atmospheric columnar aerosol concentration (kg m^{-2}) can be derived from the aerosol optical depth (AOD), the fine mode fraction (η) and r_{eff} through a recent algorithm developed by Gassó and Hegg (*44*). The mass concentration at sea level, or total suspended particle matter (TSP, kg m^{-3}), is obtained, assuming a relative humidity correction to the remotely sensed data, the same used to parametrize v_D (Annex III) and assuming that the aerosol is located and distributed homogeneously in the ABL (first 1000 m of air over the ocean). This last assumption results from the fact that satellite measurements are air-column integrated, and the variability of the vertical profiles of aerosols, which have a layered structure (*45*). However, the above assumption is consistent with the tendency of aerosols in the ABL over open oceans

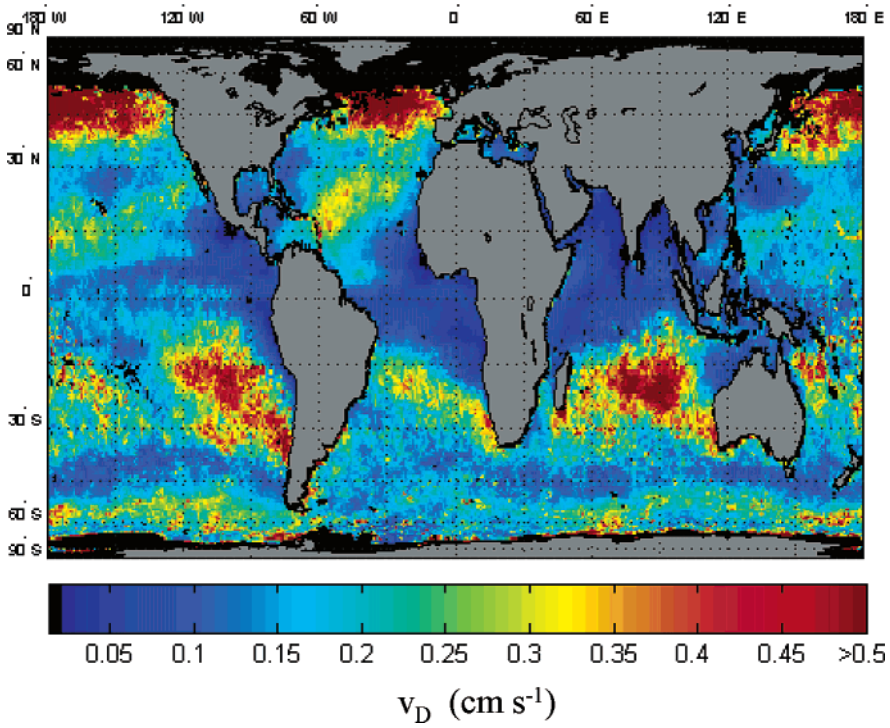

FIGURE 2. Map of overall dry deposition velocity (v_D) for the global Oceans. Values are referred to January 2001.

to be homogeneously mixed (*31*). Oceanic TSP values for November 2002−2003 are shown in Figure 1. Higher aerosol mass concentrations are found in the mid-high latitudes of the SH and in the dust outflow regions. Lower values are located along the Intertropical Convergence Zone (ITCZ), presumably due to the important role of precipitation scavenging in this region.

POP partitioning to aerosols has been described using two different sorption mechanisms: absorption into the organic phase of aerosols and adsorption onto soot carbon, as described elsewhere (*46*−*49*). The former has been successfully employed to model aerosol−gas partitioning of a wide range of POPs, such as PCBs and polychlorinated naphthalenes (PCNs), using the octanol−air partition coefficient (K_{OA}, dimensionless) as a predictor of the gas-organic matter partitioning. Due to the difficulty in determining the fraction of aerosol organic carbon from remote sensing measurements, a value of 15% has been considered representative over the oceans, consistent with measurements in open ocean (*12*, *50*). In the present paper, K_P values determined experimentally for PCDD/Fs have been used, except in the seasonal trends section for the January, April, and July estimations. For example, K_P values ranged between 2×10^{-3} and 2×10^{-1} for Cl_5DD and between 2×10^{-2} and 4×10^{-1} for OCDD. Adsorption onto the soot fraction of atmospheric aerosols may be an important mechanism affecting the gas-phase partitioning of PCDD/Fs, as has been observed for PAHs (*49*), but not so important for most PCBs. In this case, the K_P is driven not only by absorption into the organic matter (K_{OA}) but also to adsorption onto the soot phase (soot/air partition coefficient K_{SA}, $m^3\ kg^{-1}$), with elemental carbon being a surrogate for soot. It has been assumed a ratio OC/EC of 5, in agreement with measures in marine and remote areas (*31*, *34*).

Gas Absorption and Net Air−Water Exchange Fluxes. Net diffusive gas-exchange (or dry gaseous deposition) is driven by the concentration gradient across the air−sea interface and depends strongly on wind speed, temperature, and compound specific physical-chemical properties, which all influence the mass transfer coefficient (k_{AW}, m d^{-1}). Absorption (F_{AW_abs}, pg m^{-2} d^{-1}) and volatilization fluxes (F_{AW_vol}, pg m^{-2} d^{-1}) are computed respectively by

$$F_{AW\_abs} = k_{AW}\frac{C_G}{H'} \quad (8)$$

$$F_{AW\_vol} = k_{AW}C_W \quad (9)$$

where C_W is the POP dissolved-phase concentration (pg m^{-3}) and H′ (dimensionless) is the temperature and salinity corrected Henry's law constant. The net air−water exchange flux (F_{AW}, pg m^{-2} d^{-1}) is given by the difference of absorption and volatilization fluxes. C_W values have been obtained by applying a model that couples air−water exchange, phytoplankton uptake, and settling of organic matter as described by Dachs et al. (*5*). This parametrization has been successfully applied in previous studies (*5*, *9*). On the other hand, k_{AW} has been estimated in the traditional manner, as the result of the transfer through two films at each side of the air−water interface (see refs *52* and *53*), and using monthly mean sea surface temperature and wind speed determined by remote sensing. The assumption of a Weibull distribution of wind speed has been used to account for the nonlinear influence of this wind speed on k_{AW} (*5*).

Results and Discussion

Dry Aerosol Deposition and Net Air−Water Exchange Fluxes. Dry aerosol deposition and gross and net air−water exchange fluxes have been estimated using the measured atmospheric concentrations (*16*, *17*) and remote sensing meteorological data, as reported in the Data Sources and Model Development sections discussed above. The measured latitudinal profiles of gas-phase concentrations of PCDD/Fs and PCBs and the measured and predicted aerosol-phase concentrations of PCDD/Fs and PCBs have been considered representative of the whole longitudinal width of the Atlantic when computing the average dry depositional fluxes.

The averaged latitudinal profiles of dry deposition and net air−water exchange fluxes for the Atlantic Ocean are shown in Figure 3. Results are shown for two PCDD/Fs homologue groups (Cl_5DDs and OCDF) and PCBs (PCB 52

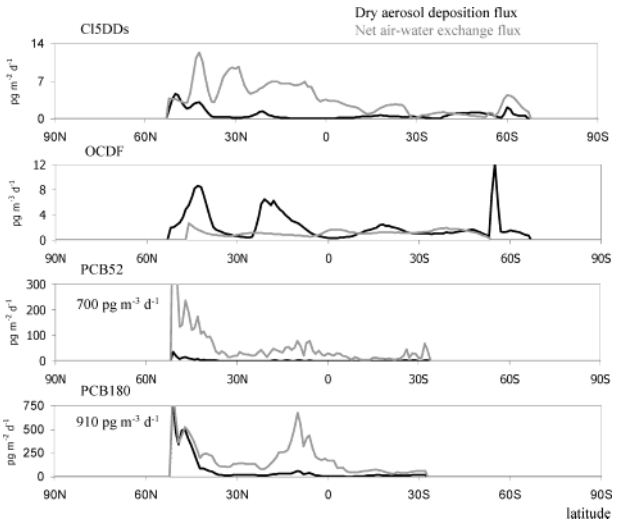

FIGURE 3. Latitudinally averaged profile of the dry aerosol deposition and net air−water exchange fluxes for Cl_5DDs, OCDF, PCB52, and PCB180 in the Atlantic Ocean. Zero values are shown for regions where satellite and/or POP measurements are not available.

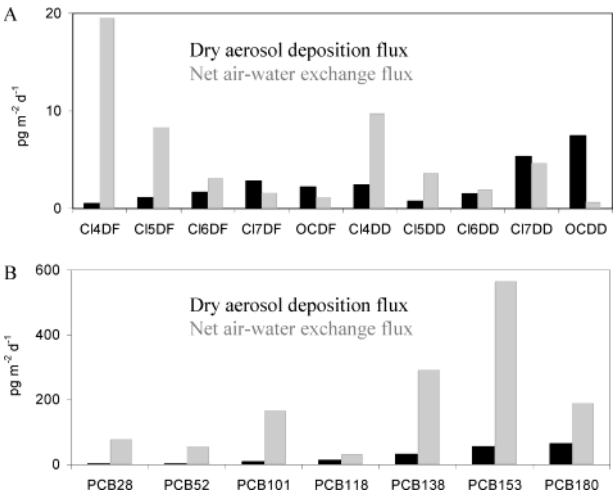

FIGURE 4. Comparison of mean dry aerosol deposition and air−water exchange fluxes for PCDD/Fs homologue groups (A) and PCBs (B) for the Atlantic Ocean.

and PCB 180) with different physical-chemical properties. There is a substantial variability in the calculated fluxes, highlighting the importance of considering spatially resolved data for global assessments of POP cycling. The dry deposition fluxes increase at mid-high latitudes, where temperatures are lower and contaminants tend to partition to a greater extent to aerosols. Wind speeds also tend to be higher at mid-high latitudes, contributing to enhanced turbulent driven deposition of accumulation mode aerosols (0.1−1 μm). Relatively high dry deposition fluxes are projected between 10° N and 25° N, the zone influenced by the Saharan-Sahel dust. Enhanced dry deposition fluxes are also estimated around 30° S, where there are high concentrations of marine aerosol. The assumption of uniformly distributed POPs over the aerosol size range may have some influence on these results. Presumably, organic carbon content in dust aerosol is low, and therefore this could mean that the fluxes presented here in dust outflow regions are overestimated. However, dust concentrations are significantly underestimated by satellite retrievals, as discussed above, and this could counteract the assumption on OC content in large aerosols. Conversely, marine aerosols may have very low concentrations of soot, and therefore this would lead to an overestimation of aerosol-phase concentrations of PCDD/Fs, but not of PCBs, and the associated dry aerosol deposition fluxes. Further research is needed on gas-particle partitioning of POPs for different types of aerosols in order to improve the accuracy of deposition estimates.

In contrast to the dry deposition flux, net air−water exchange shows a distinct latitudinal profile. The diffusive air−water exchange flux is mainly driven by temperature, wind speed, and sinking fluxes, the latter being favored in areas of high primary productivity (5). PCBs also exhibit relatively high air−water exchange fluxes at high latitudes, due to the combined effect of wind speed and primary productivity. In the NH, greater fluxes are also driven by higher gas- and aerosol-phase concentrations due to the proximity of sources. The percentage contribution of the dry aerosol deposition flux to the total depositional flux (i.e., dry aerosol deposition + net air−water exchange) is shown for selected PCBs and PCDD/Fs in Table 1. It varies from 2 to 27% and from 4 to 71% for PCBs and PCDD/Fs, respectively, with higher contributions at high latitudes and for the less volatile POPs.

Average dry aerosol deposition and net air−water exchange fluxes for the Atlantic Ocean are shown in Figure 4 for all the PCDD/Fs and selected PCB congeners. Averaged dry aerosol deposition fluxes are in the order of 1−7 pg m^{-2} d^{-1} for PCDD/Fs and 2−64 pg m^{-2} d^{-1} for PCBs. Net air−water exchange fluxes were more than 20 times higher than dry aerosol deposition fluxes for Cl_4DD/Fs but decreased with increasing chlorination level. For $Cl_{7-8}DD/Fs$, dry aerosol deposition dominates over the net air−water exchange flux. By contrast, averaged net air−water exchange was higher than the dry aerosol deposition flux for all PCBs. This is consistent with the higher fraction of PCBs in the gas phase and the affinity of PCDD/Fs to soot aerosol carbon. An important spatial variability was encountered; although air−water exchange is the main transfer route from the atmosphere to oceans for PCBs, this was not the case in some regions (see discussion below). If the gross gaseous absorption flux is considered instead of the net air−water exchange (absorption − volatilization), then its average magnitude to the Atlantic Ocean would be about 3−5-fold higher than the air−water exchange flux for PCBs and 2−3-fold higher for PCDD/Fs

TABLE 1. Averaged Percentage of Dry Aerosol Deposition Flux to the Atlantic versus Sum of Net Air−Water Exchange Flux and Dry Aerosol Deposition Fluxes

	(51° N, 1° E)−(75° S, 20° W)			(52° N, 1° E)−(34° S, 20° E)		
Fdd*100/ (Fdd+Faw)	Cl_5DDs	Cl_6DDs	OCDF	PCB52	PCB101	PCB180
60° N-90° N	NM[a]	NM[a]	NM[a]	NM[a]	NM[a]	NM[a]
30° N-60° N	17	59	71	4	5	27
0° −30° N	4	14	66	2	3	10
30° S-0°	17	27	47	3	4	13
60° S-30° S	39	55	46	6	7	23
90° S-60° S	22	ND[b] & NM[a]	ND[b] & NM[a]	NM[a]	NM[a]	NM[a]

[a] NM: not measured. [b] ND: not detected.

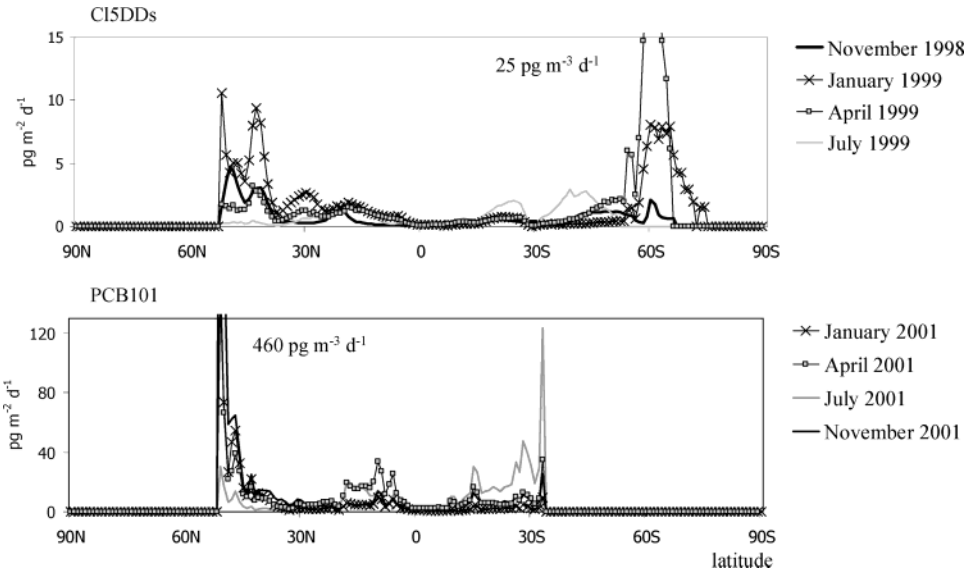

FIGURE 5. Estimated dry aerosol deposition fluxes for Cl_5DDs and PCB 101 for January, April, July, and November 1998−1999 for the Atlantic Ocean. Zero values are shown for regions where satellite and/or POP measurements are not available.

(see Figure 4 and Annex IV in Supporting Information). Still, even if gross fluxes are considered, dry aerosol deposition plays a significant role for some oceanic regions and especially for OCDD. The dominant role of diffusive fluxes in comparison with deposition of aerosol bound compounds may be the dominant trend for most atmospheric organic compounds, especially those found predominantly in the gas phase.

Comparison with Measurements. To validate the methodology described above, direct measures of dry aerosol deposition fluxes were compared with the estimated fluxes. The studies that report dry deposition fluxes of PCBs and PCDD/Fs are for continental regions, and there are only a few measurements and estimations for coastal zones and islands. No measurements appear to have been reported in remote oceanic regions. The most representative reported measurements for oceanic regions are those of van Drooge et al. (*54*, *55*), who reported dry aerosol deposition fluxes of 320 ng m^{-2} y^{-1} for the sum of PCB congeners 28, 52, 101, 118, 138, 153, and 180 to the Tenerife Island in the NE subtropical Atlantic. These values were a factor of 2 higher than the fluxes estimated here (180 ng m^{-2} y^{-1}) within a window of 3° × 3° around the sampling site, using the gas-phase concentrations reported in van Drooge et al. (*54*, *55*). Comparison of the results estimated in the present study, which are for open ocean regions, may be biased in comparison to those reported in more impacted regions. Indeed, the average dry deposition flux of 66 ng ∑PCB m^{-2} yr^{-1} estimated for the Atlantic Ocean in this study is about 1 order of magnitude lower than typical results measured in coastal areas such as Galveston Bay in Texas (4900 ng m^{-2} yr^{-1} (*56*)), or estimated by mass balance for Lake Superior (3600 ng m^{-2} yr^{-1} (*57*)), or using the hybrid-receptor deposition modeling approach in Lake Michigan (660 ng m^{-2} yr^{-1} (*58*)).

Baker and Hites (*17*) estimated the dry deposition of particulate PCDD/Fs based on air samples taken in Barbados and Bermuda, assuming $v_D = 0.3$ cm s^{-1}. Their calculated dry aerosol deposition flux to the oceans were 1.5 ± 0.6 pg m^{-2} d^{-1}, well within the range of values calculated here based on latitudinally varying atmospheric concentrations (*12*, *13*). Estimated dry deposition values of PCDD/Fs are also lower than measured dry particle fluxes over terrestrial environments. The estimated average flux of 9 ng m^{-2} yr^{-1} for the Atlantic Ocean falls in the lower range of the measured fluxes in rural Bloomington (0.3−37 ng m^{-2} yr^{-1} (*2*)) and is much lower than in impacted areas of Japan (230 ng m^{-2} yr^{-1} (*59*)).

The pattern of an increasing contribution of heavier congeners in particulate deposition fluxes was consistent with other studies (*60*). Previous estimations of global oceanic depositional fluxes of PCBs were performed in a pioneering study published in 1991 by Duce et al. (*61*) which, as in this paper, used a climatological approach to estimate the fluxes. Duce et al. (*47*) estimated dry aerosol deposition fluxes 3-fold lower than in the present study, because they assumed lower deposition velocities due to a lack of aerosol size distribution information. Conversely, their net air−water exchange fluxes were about 3.5 times higher than the estimates here. The current state-of-the art allows for better precision and resolution in atmospheric deposition estimations. Both studies highlight the important role that diffusive exchange plays in the global dynamics of POPs.

The total dry aerosol deposition of PCBs and PCDD/Fs to the Atlantic Ocean is estimated here to be 2200 kg yr^{-1} and 500 kg yr^{-1}, respectively. The net air−water exchange is significantly higher, about 22000 kg ΣPCB yr^{-1} for PCBs and 1300 kg ΣPCDD/Fs yr^{-1}. There is a need for measurements of depositional fluxes of PCBs, PCDD/Fs, and other POPs to remote oceanic regions to obtain a better picture of their role as global sinks for POPs. However, until those are available, the estimations reported here indicate the importance of these fluxes to the Atlantic and provide a methodology that can be applied at the global or regional scale elsewhere.

Seasonal Trends of Dry Deposition Fluxes. Some meteorological variables, such as wind speed and temperature are strongly seasonal and can influence the shape and magnitude of the mass aerosol distribution. Seasonal variability in the latitudinal distribution of dry deposition fluxes was assessed by comparing four months: January, April, July, and November. It was assumed that gas-phase concentrations do not show a temperature dependence, as observed in recent measurements in the Canary Islands and in the eastern Mediterranean, consistent with the fact that atmospheric concentrations over the oceans are usually the result of LRAT (*54*, *62*). For those months when field measurements were not available, aerosol-phase concentrations of PCBs and PCDD/Fs were predicted from temperature-dependent K_P values as described above. Figure 5 shows the latitudinal profiles of dry, aerosol and gaseous, deposition fluxes for Cl_5DDs and PCB 101 to the Atlantic Ocean.

Marked seasonality in dry aerosol deposition fluxes was estimated at mid and high latitudes, while low or no seasonal variability occurred between the tropics. Variability was highest toward high latitudes in both hemispheres, where temperature and wind speed are seasonally dependent and lowest/highest during cold periods, respectively. Dry aerosol deposition is therefore enhanced due to two combined effects. Higher wind speeds increase deposition velocities of accumulation mode aerosols (see Annex III) and modulate strongly marine aerosol concentrations over the sea surface (*63*, *64*). Lower temperatures increase the fraction of atmospheric POPs bound to aerosols, thus increasing the depositional flux. Furthermore, some variability is observed between 10° N and 25° N, due to the seasonality of the Saharian-Sahel dust outflow over the Atlantic. Dust storms are active nearly all year but with varying spatial coverage and peaking during warm season (March−August) (*65*).

Dominant Atmospheric Depositional Mechanism to the Global Oceans. In addition to assessing the relative importance of dry deposition and air−water exchange for the Atlantic, it is interesting to identify the dominant atmospheric deposition process for oceans globally. Pollutant input fluxes to the surface ocean are given by the product of two terms: a kinetic parameter, or mass transfer coefficient, and the aerosol-bound or the gas-phase POP concentration. Absorption and dry aerosol deposition fluxes are depositional processes behaving in parallel. An analogy can be set between the transfer of pollutants from the atmosphere to the ocean and two electrical resistances in parallel, namely the mass transfer coefficient is the inverse of the resistance (*66*). Hence, for a given amount of pollutant in the atmosphere (represented either by the gas-phase or the particle-phase concentration), the preferred transport mechanism to the surface ocean will be associated with the lower resistance, i.e., greater mass transfer coefficient. To assess the dominant fluxes at the global scale, mass transfer coefficients were compared, derived globally from remote sensing measurements as explained before. In other words, this comparison shows the tendency of a contaminant to either deposit via aerosol deposition or via gas exchange independently of the actual POP occurrence in the gas and aerosol phases.

For diffusive absorption the mass transfer coefficient is given by k_{AW}/H' (see eq 8), which is the accompanying term of the concentration in the gaseous phase. However, the dry aerosol deposition flux given by eq 1 is related to particle-phase concentrations, and therefore its mass transfer coefficient (the dry deposition velocity v_D) cannot be compared directly. The aerosol deposition flux needs to be related to the gas-phase concentration, by using the particle-gas partitioning models. Reordering eq 1, then

$$F_{DD} = v_D \frac{\phi}{(1-\phi)} \times C_G \qquad (10)$$

where ϕ (dimensionless) is the fraction of the atmospheric POP concentration which is aerosol-bound (C_P/C_P+C_G). It can be estimated from gas-particle partitioning models by

$$\phi = \frac{K_p(TSP)}{1 + K_p(TSP)} \qquad (11)$$

The extent of POP association to aerosols depends on several factors, namely compound vapor pressure, the ambient air temperature, and the amount and type of aerosol present. ϕ values were estimated using eq 11 for PCBs but determined using measured field C_G and C_P concentrations for PCDD/Fs.

The dominant flux was therefore assessed by determining which of the mass transfer coefficients is greater, k_{AW}/H' or $(v_D\,\phi)/(1-\phi)$. Figure 6 shows the ratio of mass transfer velocity

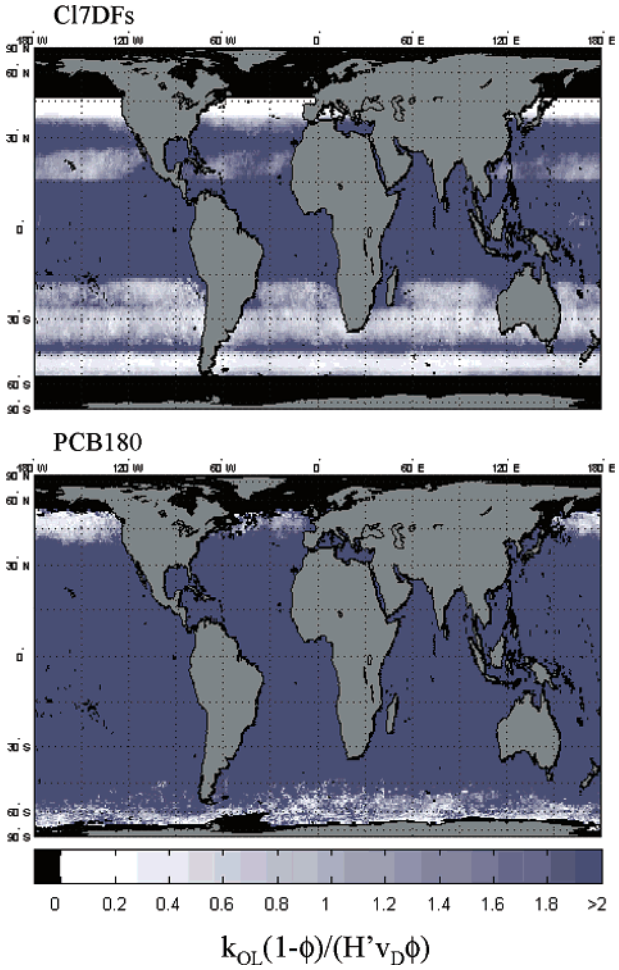

FIGURE 6. Ratio between mass transfer velocity of diffusive absorption and dry deposition velocity, for Cl_7DFs (A) and PCB 180 (B). Values greater than 1 indicate air−water exchange dominates, while values lower than 1 indicate dry aerosol deposition as the dominant depositional mechanism.

of absorption to dry deposition for two high chlorinated POPs: Cl_7DFs and PCB180. When the ratio < 1, dry aerosol deposition dominates; diffusive air−water exchange dominates the total atmospheric deposition over the ocean when the ratio > 1. Figure 6 shows that gaseous absorption generally dominates over dry aerosol deposition—even for these heavier compounds. However, values < 1 occur in some regions for some compounds under the following meteorological conditions: high wind speeds, larger aerosol diameters, low temperatures, and high TSP values. In short, dry deposition velocities become more important at higher latitudes, as discussed above for the Atlantic Ocean. What is striking is that the dominance of dry aerosol deposition over diffusive absorption is higher in the SH. This trend may be because high wind speeds, high TSP, and raised aerosol diameters are found in the southern ocean and markedly during April−July. The MODIS sensor does not differentiate between dust and marine aerosols, and thus the significant fluxes observed in the southern ocean (with high wind speeds) suggest that marine aerosol may play an important role enhancing dry deposition of POPs. This mechanism needs further research.

PCBs are found mainly in the gas phase. The results found in this study therefore suggest that air−water exchange is the dominant depositional process for PCBs in most environments. This is consistent with other studies at local or regional scales and assessments of global cycling of PCBs that consider air−water exchange as the dominating depositional process (*5*). Conversely, PCDD/Fs show a higher

affinity to aerosols, presumably due to a significant effect of aerosol soot carbon (*67*). Hence, for the high chlorinated PCDD/Fs, dry deposition is the dominant process in many oceanic regions. PAHs show an even stronger affinity to aerosols due to soot carbon (*34*, *49*), and thus dry aerosol deposition of most four to six ring PAHs may be dominated by dry deposition in most oceanic areas. An important result of the present study is the spatial variability of both air−water exchange and dry aerosol deposition at the regional and global scale. This needs to be taken into account when assessing the environmental fate of POPs at regional and global scales. Finally, dry aerosol deposition will be specially relevant in dust and marine aerosol influenced areas.

Acknowledgments

The satellite data used in this study were acquired as part of the NASA's Earth Science Enterprise. The algorithms were developed by the MODIS Science Teams. The data were processed by the MODIS Adaptive Processing System (MODAPS) and Goddard Distributed Active Archive Center (DAAC) and are archived and distributed by the Goddard DAAC. NOAA and ATSR processing teams are also acknowledged. The authors appreciate useful comments made by Santiago Gassó (GESTC/U. Maryland). This work was supported by the Spanish Ministry of Science and Technology through project AMIGOS (REN2001-3462/CLI).

Supporting Information Available

Further details on cruise data and methodology to estimate dry deposition velocities (Annexes I, II, and III) and comparison of gross gaseous absorption and dry aerosol deposition fluxes (Annex IV). This material is available free of charge via the Internet at http://pubs.acs.org.

Literature Cited

(1) Wania, F.; Axelman, J.; Broman, D. *Environ. Pollut.* **1998**, *102*, 3−23.
(2) Eitzer, B. D.; Hites, R. A. *Environ. Sci. Technol.* **1989**, *23*, 1396−1401.
(3) Lipiatou, E.; Albaigés, J. *Mar. Chem.* **1994**, *46*, 153−164.
(4) Baker, J. I.; Hites, R. A. *Environ. Sci. Technol.* **1999**, *33*, 14−20.
(5) Dachs, J.; Lohmann, R.; Ockenden, W. A.; Méjanelle, L.; Eisenreich, S. J.; Jones, K. C. *Environ. Sci. Technol.* **2002**, *36*, 4229−4237.
(6) Van Jaarsveld, J. A.; Van Pul, W. A. J.; De Leeuw, F. A. A. M. *Atmos. Environ.* **1997**, *31*, 1011−1024.
(7) Scheringer, M.; Salzmann, M.; Stroebe, M.; Wegmann, F.; Fenner, K.; Hungerbühler, K. *Environ. Pollut.* **2004**, *128*, 177−188.
(8) Wania, F.; Mackay, D. *Environ. Sci. Technol.* **1996**, *30*, 390A−396A.
(9) Dachs, J.; Eisenreich, S. J.; Baker, J. E.; Ko, F.-C.; Jeremiason, J. D. *Environ. Sci. Technol.* **1999**, *33*, 3653−3660.
(10) Palm, A.; Cousins, I.; Gustafsson, O.; Axelman, J.; Grunder, K.; Broman, D.; Brorstrom-Lunden, E. *Environ. Pollut.* **2004**, *128*, 85−97.
(11) Gigliotti, C. L.; Brunciak, P. A.; Dachs, J.; Glenn, T. R.; Nelson, E. D.; Totten, L. A.; Eisenreich, S. J. *Environ. Toxicol. Chem.* **2002**, *21*, 235−244.
(12) Heintzenberg, J.; Covert, D. C.; Van Dingenen, R. *Tellus* **2000**, 1104−1122.
(13) Kaufman, Y. J.; Tanré, D.; Boucher, O. *Nature* **2002**, *419*, 215−223.
(14) Shatalov, V.; Dutchak, S.; Fedyunin, M.; Mantseva, E.; Strukov, B.; Varygina, M.; Vulykh, N.; Aas, W.; Mano, S. *Persistent Organic Pollutants in the Environment*; EMEP Status Report 3/2003; 2003.
(15) Jones, K. C.; de Voogt, P. *Environ. Pollut.* **1999**, *100*, 209−221.
(16) Lohmann, R.; Ockenden, W. A.; Shears, J.; Jones, K. C. *Environ. Sci. Technol.* **2001**, *35*, 4046−4053.
(17) Jaward, F. M.; Barber, J. L.; Booij, K.; Dachs, J.; Lohmann, R.; Jones, K. C. *Environ. Sci. Technol.* **2004**, *38*, 2617−2625.
(18) Remer, L. A.; Tanré, D.; Kaufman, Y. J.; Ichoku, C.; Mattoo, S.; Levy, R. C.; Chu, D. A.; Holben, B. N.; Dubovik, O.; Smirnov, A.; Martins, J. V.; Li, R.-R.; Ahmad, Z. *Geophys. Res. Lett.* **2002**, *29*, 1618.
(19) Levy, R. C.; Remer, L. A.; Tanré, D.; Kaufman, Y. J.; Ichoku, C.; Holben, B. N.; Livingston, J. M.; Russell, P. B.; Maring, H. *J. Geophys. Res.* **2003**, *108*, 8594.
(20) Kinne, S.; Lohmann, U.; Feitchter, J.; M., S.; Timmreck, C.; Ghan, S.; Easter, R.; Chin, M.; Ginoux, P.; Takemura, T.; Tegen, I.; Koch, D.; Herzog, M.; Penner, J. E.; Pitari, G.; Holben, B. N.; Eck, T.; Smirnov, A.; Dubovik, O.; Slutsker, I.; Tanré, D.; Torres, O.; Mishchenko, M.; Geogdzhayev, I.; Chu, D. A.; Kaufman, Y. J. *Monthly averages of aerosol properties: A global comparison among models, satellite sata and AERONET ground data*; MPI for Meteorology: 2003.
(21) McVeety, B. D.; Hites, R. A. *Atmos. Environ.* **1988**, *22*, 511−536.
(22) Williams, R. M. *Atmos. Environ.* **1982**, *16*, 1933−1938.
(23) Slinn, S. A.; Slinn, W. G. N. *Atmos. Environ.* **1980**, *14*, 1013−1016.
(24) Ondov, J. M.; Quinn, T. L.; Battel, G. F. Influence of temporal changes in relative humidity on size and dry depositional fluxes of aerosol particles bearing trace elements. In *Atmospheric deposition of contaminants to the great lakes and coastal waters. Precedings from a session at the SETAC 15th Annual Meeting 30 October-4 November 1994*; Baker, J. E., Ed.; SETAC Press: Denver, 1994; pp 17−34.
(25) Shatalov, V.; Fedyunin, M.; Mantseva, E.; Strukov, B.; Vulykh, N. *Persistent Organic Pollutants in the Environment;* MSC-E Technical Report 4/2003; MSC-E, 2003.
(26) Nho-Kim, E.-Y.; Michou, M.; Peuch, V.-H. *Atmos. Environ.* **2004**, *38*, 1933−1942.
(27) J. Zufall, M.; Dai, W.; I. Davidson, C. *Atmos. Environ.* **1999**, *33*, 4283−4290.
(28) Zufall, M. J.; Davidson, C. I. Dry deposition of particles to water surfaces. In *Atmospheric deposition of contaminants to the great lakes and coastal waters. Proceedings from a session at the SETAC 15th Annual Meeting 30 October-4 November 1994*; Baker, J. E., Ed.; SETAC Press: Denver, 1994; pp 1−15.
(29) Holsen, T. M.; Noll, K. E. *Environ. Sci. Technol.* **1992**, *26*, 1807−1815.
(30) Caffrey, P. F.; Ondov, J. M.; Zufall, M. J.; Davidson, C. I. *Environ. Sci. Technol.* **1998**, *32*, 1615−1622.
(31) Seinfeld, J. H.; Pandis, S. N. *Atmospheric chemistry and physics: From air pollution to climate change*; Wiley-Interscience: New York, 1998.
(32) Kaufman, Y. J.; Tanré, D.; Gordon, H. R.; Nakajima, T.; Lenoble, J.; Frouin, R.; Grassl, H.; Herman, B. M.; King, M. D.; Teillet, P. M. *J. Geophys. Res.* **1997**, *102*, 16815−16830.
(33) Hansen, J. E.; Travis, L. D. *Space Sci. Rev.* **1974**, *16*.
(34) Lohmann, R.; Lammel, G. *Environ. Sci. Technol.* **2004**, *38*, 3793−3803.
(35) Poster, D. L.; Baker, J. E. *Environ. Sci. Technol.* **1996**, *30*, 349−354.
(36) Kaupp, H.; McLachlan, M. S. *Atmos. Environ.* **2000**, *34*, 73−83.
(37) Miguel, A. H.; Eiguren-Fernandez, A.; Jaques, P. A.; Froines, J. R.; Grant, B. L.; Mayo, P. R.; Sioutas, C. *Atmos. Environ.* **2004**, *38*, 3241−3251.
(38) Simcik, M. F. Fate and transport of polychlorinated biphenyls and polycyclic aromatic hydrocarbons in Chicago/Lake michigan. Ph.D. Thesis, Graduate School-New Brunswick Rutgers, New Brunswick, 1998.
(39) Chen, S.-J.; Liao, S.-H.; Jian, W.-J.; Lin, C.-C. *Environ. Int.* **1997**, *23*, 475−488.
(40) Holsen, T. M.; Noll, K. E.; Liu, S.-P.; Lee, W.-J. *Environ. Sci. Technol.* **1991**, *25*, 1075−1081.
(41) Livingstone, D. M.; Imboden, D. M. *Tellus* **1993**, *45B*, 275−295.
(42) Holsen, T. M.; Noll, K. E.; Fang, G.-C.; Lee, W.-J.; Lin, J.-M. *Environ. Sci. Technol.* **1993**, *27*, 1327−1333.
(43) Pankow, J. F. *Atmos. Environ.* **1994**, *28*, 185−188.
(44) Gassó, S.; Hegg, D. A. *J. Geophys. Res.* **2003**, *108*, 4010−4035.
(45) Collins, D. R.; Jonsson, H. H.; Seinfeld, J. H.; Flagan, R. C.; Gassó, S.; Hegg, D. A.; Russell, P. B.; Schmid, B.; Livingston, J. M.; Öström, E.; Noone, K. J.; Russell, L. M.; Putaud, J. P. *Tellus* **2000**, *52B*, 498−525.
(46) Harner, T.; Bidleman, T. *Environ. Sci. Technol.* **1998**, *32*, 1494−1502.
(47) Bucheli, T. D.; Gustafsson, O. *Chemosphere* **2003**, *53*, 515−522.
(48) Harner, T.; Bidleman, T. *J. Chem. Eng. Data* **1998**, *43*, 40−46.
(49) Dachs, J.; Eisenreich, S. J. *Environ. Sci. Technol.* **2000**, *34*, 3690−3697.
(50) Raes, F.; Bates, T.; McGovern, F.; Van Liedeker, M. *Tellus* **2000**, *2000*, 111−125.
(51) Totten, L. A.; Brunciak, P. A.; Gigliotti, C. L.; Dachs, J.; Glenn, T. R.; Nelson, E. D.; Eisenreich, S. J. *Environ. Sci. Technol.* **2001**, *35*, 3834−3840.
(52) Nightingale, P. D.; Liss, P. S.; Schlosser, P. *Geophys. Res. Lett.* **2000**, *27*, 2117−2120.
(53) Nightingale, P. D.; Malin, G.; Law, C. S.; Watson, A. J.; Liss, P. S.; Liddicoat, M. I.; Boutin, J.; Upstill-Goddard, R. C. *Global Biogeochem. Cycles* **2000**, *14*, 373−387.
(54) Van Drooge, B. L.; Grimalt, J. O.; Torres-Garcia, C. J.; Cuevas, E. *Environ. Sci. Technol.* **2002**, *36*, 1155−1161.

(55) Van Drooge, B. L.; Grimalt, J. O.; Torres-Garcia, C. J.; Cuevas, E. *Mar. Pol. Bull.* **2001**, *42*, 628−634.
(56) Park, J.-S.; Wade, T. L.; Sweet, S. *Atmos. Environ.* **2001**, *35*, 3315−3324.
(57) Swackhamer, D. L.; McVeety, B. D.; Hites, R. A. *Environ. Sci. Technol.* **1988**, *22*, 664−672.
(58) Pirrone, N.; Keeler, G. J.; Holsen, T. M. *Environ. Sci. Technol.* **1995**, *29*, 2123-2132.
(59) Hirai, Y.; Sakai, S.-i.; Watanabe, N.; Takatsuki, H. *Chemosphere* **2003**, *54*, 1383−1400.
(60) Schröder, J.; Welsch-Pausch, K.; McLachlan, M. S. *Atmos. Environ.* **1997**, *31*, 2983−2989.
(61) Duce, R. A.; Liss, P. S.; Merrill, J. T.; Atlas, E. L.; Buat-Menard, P.; Hicks, B. B.; Miller, J. M.; Prospero, J. M.; Arimoto, R.; Church, T. M.; Ellis, W.; Galloway, J. N.; Hansen, L.; Jickells, T. D.; Knap, A. H.; Reinhardt, K. H.; Schneider, B.; Soudine, A.; Tokos, J. J.; Tsunogai, S.; Wollast, R.; Zhou, M. *Global Biogeochem. Cycles* **1991**, *5*, 193−259.
(62) Mandalakis, M.; Stephanou, E. G. *J. Geophys. Res.* **2002**, *107*, 4716−4726.
(63) Gong, S. L.; Barrie, L. A.; Prospero, J. M.; Savoie, D. L.; Ayers, G. P.; Blanchet, J.-P.; Spacek, L. *J. Geophys. Res.* **1997**, *102*, 3819−3830.
(64) O'Dowd, C. D.; Smith, M. H. *J. Geophys. Res.* **1993**, *98*, 1137−1149.
(65) Brooks, N.; Legrand, M. Dust variability over northern Africa and rainfall in the Sahel. In *Linking Climate Change to Land Surface Change*; Kluwer Academic Publishers: Dordrecht, 2000; pp 1−25.
(66) Schwarzenbach, R. P.; Gschwend, P. M.; Imboden, D. M. *Environmental organic chemistry*, 2nd ed.; Wiley-Interscience: 2000.
(67) Lohmann, R.; Harner, T.; Thomas, G. O.; Jones, K. C. *Environ. Sci. Technol.* **2000**, *34*, 4943−4951.

Received for review May 21, 2004. Revised manuscript received August 5, 2004. Accepted August 16, 2004.

ES049240V